Journal of Thermal Analysis, Vol. 38 (1992) 2301-2310

KINETIC ANALYSIS OF THERMOGRAVIMETRIC DATA
XXVIII Thermal decomposition of some metal and ammonium salts of hexabromoplatinic acid

G. Liptay, J. Zsakó**, Cs. Várhelyi*** and Cs. Novák**

*FACULTY OF CHEMISTRY, TECHNICAL UNIVERSITY, BUDAPEST, H-1521
HUNGARY
**FACULTY OF CHEMICAL TECHNOLOGY, 'BABES-BOLYAI' UNIVERSITY, CLUJ,
R-3400 ARANY JÁNOS STREET 11, ROMANIA
***DEPTMENT OF NATURAL SCIENCES AND MATHEMATICS, TRANSYLVANIAN
MUSEUM ASSOCIATION, CLUJ, ROMANIA

(Received July 18, 1991)

The potassium, ammonium and thirteen amine salts of hexabromoplatinic acid were obtained and characterized by chemical analysis. The thermal decompositions of these complex salts were studied by derivatograph and differential scanning calorimetry. The natures of the pyrolysis processes are discussed and compared with those obtained for the analogous chlorocomplexes. From the TG curves, kinetic parameters were derived for different stages of the thermal decomposition.

Keywords: hexabromoplatinate complexes, kinetic parameters, pyrolysis processes

Introduction

Hexabromoplatinic acid, $H_2[PtBr_6]$, can be obtained by dissolving platinum in a large excess of a mixture of conc. hydrobromic and nitric acids [1], or by repeated evaporation of an aqueous solution of $H_2[PtCl_6]$ with conc. hydrobromic acid and elementary bromine [2].

This dibasic strong complex acid forms well-defined crystalline salts with the alkali metals and some monovalent transition metals. Generally, the hexabromoplatinates of the di- and trivalent metals are less characteristic substances. A series of Co(III), Cr(III) and Rh(III)-amine complex salts of various types with

John Wiley & Sons, Limited, Chichester
Akadémiai Kiadó, Budapest

Table 1 $M_2[PtBr_6]$ and (amine·H)$_2$[PtBr$_6$]·nH$_2$O salts obtained

No.	Complex	Mol. wt. calcd.	Appearance	Analysis		
				Calcd.		Found
1	K_2A	752.9	reddish-yellow octahedral cryst.	Pt	25.93	25.86
2	$(NH_4)_2A$	710.6	reddish-yellow cubic cryst.	Pt	27.47	27.49
3	(aniline·H)$_2$A	862.7	reddish-brown long needles	Pt	22.63	22.40
				N	3.25	3.50
4	(*m*-toluidine·H)$_2$A	890.8	reddish-brown prisms	Pt	21.91	22.15
				N	3.14	3.33
5	(*m*-xylidine·H)$_2$A	918.9	gold-brown plates	Pt	21.24	21.08
6	(α-naphthylamine·H)$_2$· ·2H$_2$O	999.1	yellow-brown prisms	Pt	19.54	19.80
				N	2.80	2.65
7	(*p*-phenetidine·H)$_2$A	951.1	yellow-brown rhomb. plates	Pt	20.52	20.55
8	(pyridine·H)$_2$A	834.7	reddish-brown prisms	Pt	23.38	23.11
				N	3.36	3.42
9	(γ-picoline·H)$_2$A	862.7	reddish-brown dendrites	Pt	22.63	22.90
				N	3.24	3.11
10	(2,6-lutidine·H)$_2$A	890.8	reddish-brown square plates	Pt	21.90	21.76
				N	3.14	3.25
11	(2-methyl-5-ethyl-pyridine·H)$_2$A	918.9	reddish-brown prisms	Pt	21.24	21.10
				N	3.04	2.89
12	(benzimidazole·H)$_2$A	913.0	reddish-brown plates	Pt	21.38	21.62
13	(*o*-hydroxyquinoline·H)$_2$A· ·2H$_2$O	1003.1	gold-yellow short prisms	Pt	19.46	19.60
				N	2.79	2.57
14	(α,α'-dipyridyl·H)$_2$A· ·2H$_2$O	868.9	dark-yellow micro-cryst.	Pt	22.47	22.76
15	(*o*-phenanthroline·H$_2$)A· ·H$_2$O	875.0	dark-yellow micro-cryst.	Pt	22.31	22.51

A = [PtBr$_6$]

$H_2[PtBr_6]$ have been obtained and used for characterization of the corresponding cations [3–5].

$H_2[PtBr_6]$ gives salts with the hydrobromides of aliphatic, aromatic and heterocyclic amines, alkaloids [6, 7] and phosphines [8]. All these compounds are neutral salts. The formation of acidic salts of the type (amine·H) $H[PtBr_6]$ has not been mentioned in the available literature.

The majority of the salts $(\text{amine·H})_2$ $[PtBr_6]$ are well-defined, characteristic crystalline products, sparingly soluble in water, readily soluble in alcohol and insoluble in ether. They can be recrystallized from warm dilute hydrobromic acid, and decompose on being boiled in neutral aqueous solution, especially in the presence of NaOH.

The thermal decompositions of the free acid and the potassium salt have been studied under special conditions. It was observed, for instance, that the potassium salt decomposes to KBr, $PtBr_2$ and Br_2 on heating [9]. Some thermal data on $(\text{amine·H})_2[PtBr_6]$ are also mentioned in the literature (e.g. melting and decomposition points). The salts of this type sinter before melting, giving a resinous mass. In some cases the melting process cannot be characterized by a well-defined melting point, and is accompanied by partial decomposition [10–12].

In the present paper the potassium, ammonium and 13 amine salts of $H_2[PtBr_6]$ were obtained and their thermal behaviour studied by means of derivatography and differential scanning calorimetry. The results are compared with those obtained with the analogous salts of $H_2[PtCl_6]$ [13].

Results and discussion

The complex salts obtained from $H_2[PtBr_6]\cdot 6H_2O$ by means of double decomposition reactions with metal bromides or nitrates and with the hydrobromides of amines are characterized in Table 1.

The thermal decompositions of the studied complexes occur in several stages and the final product is always metallic platinum. The pyrolysis is simplest for the K and NH_4 salts. Their TG curves are given in Fig. 1.

As is to be seen from Fig. 1a, the potassium salt decomposes in two stages. The weight loss up to 560°C corresponds to 4 bromine atoms, i.e. the first stage consists of the following reaction:

$$K_2[PtBr_6] = Pt + 2KBr + 2Br_2$$

In the second stage the volatilization of KBr occurs. This behaviour is perfectly analogous with the pyrolysis of $K_2[PtCl_6]$, but the first stage occurs at lower temperatures for the Br derivative than for the Cl complex [13].

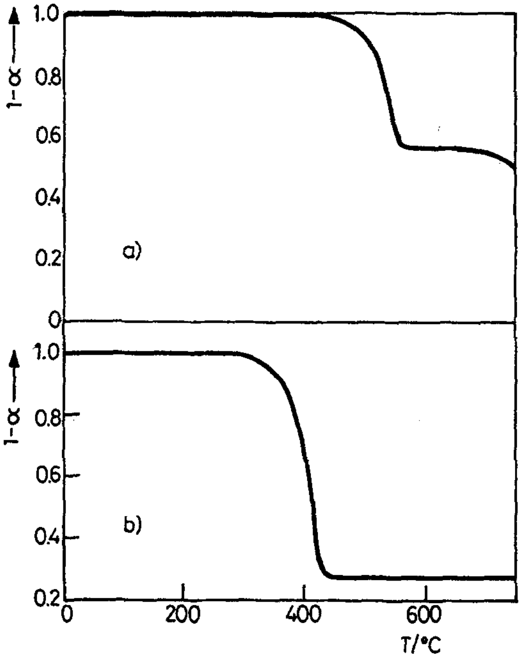

Fig. 1 TG curves of $K_2[PtBr_6]$ (*a*) and $(NH_4)_2[PtBr_6]$ (*b*)

The thermal decomposition of the ammonium salt (Fig. 1b) proceeds in a single stage, without the formation of well-defined intermediates. The pyrolysis occurs at much lower temperatures as compared with the K salt, due to the reducing character of the outer sphere NH_4^+ cation, but in about the same temperature range as for the decomposition of $(NH_4)_2[PtCl_6]$ [13]. The products of the redox reactions are gaseous ones, except the metallic platinum, and since the processes occur in the presence of atmospheric oxygen, the overall reaction may be presumed to be as follows:

$$(NH_4)_2[PtBr_6] + 1/2O_2 = Pt + N_2 + H_2O + 6HBr$$

The pyrolyses of the complexes of the type $(amine.H)_2[PtBr_6]\cdot nH_2O$ are more complicated and consist of 2–3 or even up to 6 successive stages. Several examples are given in Figs 2 and 3.

The α-naphthylamine derivative (Fig. 2) loses its crystallization water in the first, endothermal process. The second decomposition stage is also endothermal and the weight loss up to 280°C, where the process becomes exothermal, corresponds to about one mole of α-napththylamine.HBr. This is followed by 2 exothermal stages, without a clear stoichiometry. These reactions presumably occur with the participation of atmospheric oxygen. The constant weight reached at about 540°C is consistent with the conclusion that metallic Pt is the only solid product.

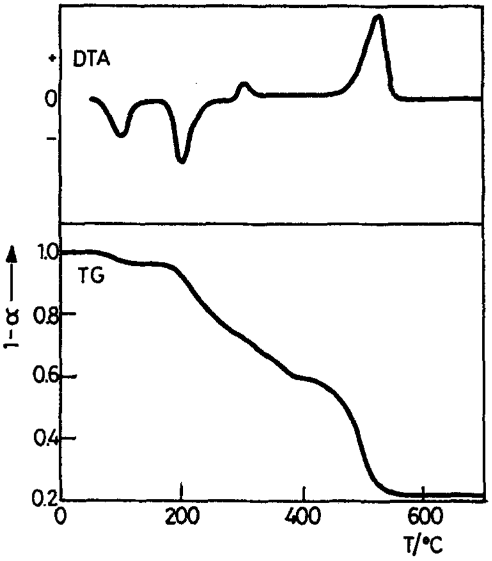

Fig. 2 TG and DTA curves of (α-naphthylamine·H)$_2$[PtBr$_6$]·2H$_2$O

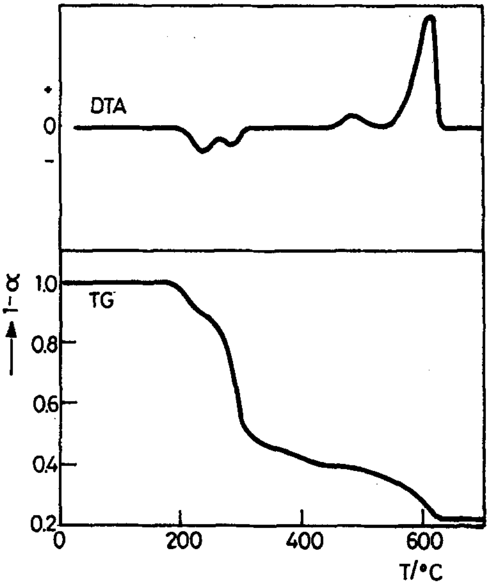

Fig. 3 TG and DTA curves of (γ-picoline·.H)$_2$[PtBr$_6$]

The γ-picoline derivative contains no crystallization water and its thermal decomposition begins at much higher temperature than that of the naphthylamine complex. The DTA curve displays 2 endothermal peaks and in the corresponding stages the weight loss exceeds 2 moles of amine·HBr. Therefore, the stoichiometry of the successive reactions cannot be observed from the TG and DTA curves. The final product is also metallic Pt in this case.

The positions of the endothermal and exothermal peaks observed in the DTA curves of the salts (amine·H)$_2$[PtBr$_6$]·nH$_2$O are given in Table 2.

Table 2 Endothermal and exothermal DTA peak temperatures in °C

Complex salt no.	Endothermal dehydration	Endothermal deamination	Exothermal
3	–	210	400
4	–	218, 240	>320
5	–	220, 265	330, 490
6	95	203	300, 520
7	–	220, 260	285, 320, ...
8	–	215, 243, 264	590
9	–	235, 285	490, 615
10	–	238, 302	345, 490
11	–	200	320, 390, 480
12	–	240	>350
13	93	190, 280	>350
14	70	198, 270, 280, 310	330, ...
15	75	196, 220, 240, 290	355, ...

Generally, the deamination endothermal peak temperatures are situated between 200° and 250°C, although the second peak may sometimes appear at higher temperatures, up to 300°–310°C. With a few exceptions, the exothermal processes occur above 300°C and they are generally finished by 450°–500°C, when the weight of the solid residue corresponds to the Pt content of the sample.

Comparison of these results with those obtained earlier with the analogous H$_2$[PtCl$_6$] derivatives [13] reveals no clear differences between the behaviour of the H$_2$[PtCl$_6$] and H$_2$[PtBr$_6$] derivatives, their pyrolyses occurring in the same temperature ranges. In this respect the above-mentioned K salts are the only exceptions.

An attempt was made to derive kinetic parameters such as apparent reaction order (n), apparent activation energy (E) and preexponential factor (Z) from some portions of the experimental TG curves. For this purpose our nomogram method [14, 15] was used. The results obtained are presented in Table 3.

Table 3 Kinetic parameters derived from the TG curves

Complex no.	Stage*	n	E/kJ	lg Z^{**}	$\tau_{0.1}$
1	$-2Br_2$	0.50	188.4	9.55	1.319
2	overall	0.75	149.4	8.90	1.580
3	exo	1.27	133.9	7.80	1.592
4	end II	3.55	415.8	42.2	2.074
4	exo I	2.24	127.4	9.54	1.890
4	exo II	2.60	255.4	14.9	1.354
5	end I	3.90	358.2	37.3	2.137
5	exo II	–0.16	74.1	1.90	1.464
6	deh	1.15	60.8	6.60	3.003
6	end	3.62	278.2	28.8	2.156
6	exo	0.42	162.8	8.46	1.375
7	end II	0.49	122.7	10.6	2.116
7	exo II	0.79	150.7	7.64	1.389
8	end II	0.35	107.5	8.50	2.092
8	exo	1.46	339.7	18.0	1.200
9	end I	0.69	136.8	11.8	2.092
10	end I	0.23	143.1	12.4	2.101
10	exo II	1.52	102.5	4.60	1.508
11	end	0.03	119.7	9.90	2.114
11	exo III	1.49	146.4	7.50	1.439
12	end	3.33	289.1	27.0	1.966
12	exo	1.09	418.7	22.3	1.167
13	deh	1.88	248.5	34.3	2.825
13	end I	0.58	87.5	7.50	2.317
13	exo	0.24	312.3	17.1	1.233
14	deh	2.12	226.8	33.4	3.021
14	end I	1.87	243.6	24.6	2.144
14	exo II	1.43	272.2	13.7	1.180
15	deh	2.43	146.5	22.1	3.195
15	end I	1.26	133.1	10.6	1.961
15	exo II	1.22	196.4	8.59	1.152

* deh – dehydration; end – endothermal deamination; exo – exothermal; I, II. III – first, second and third values in Table 2;

** Z expressed in s^{-1}

The last column of this Table gives the $\tau_{0.1} = 10^3/T_{0.1}$ value, where $T_{0.1}$ is the absolute temperature at which the conversion α attains $\alpha = 0.1$ in the decomposition stage considered.

Obviously, the kinetic parameters vary in a large interval and no correlation can be derived between their values and the characteristics of the substance decomposed. It may be observed only that the log Z values increase with increasing E, i.e. a kinetic compensation effect seems to be valid.

By using a linear regression, the parameters a and b of the linear compensation law

$$\log Z = aE + b$$

have been derived and are given in Table 4.

The kinetic compensation effect is presumed to be a consequence of the use of the Arrhenius equation. If it is presumed that a set of reactions has an isokinetic temperature T_i at which the rate constants of all the reactions are the same, the Arrhenius equation leads to the above linear compensation law, with $a = 1/2{\cdot}3RT_i$ [16, 17]. Since the rate constants must have similar values at the beginning of the thermal decomposition, it seems reasonable to take e.g. $T_{0.1}$ for T_i as a first approximation [18]. Consequently, the a value derived via linear regression of the log Z *vs.* E dependence may be expected to be very near to the $a^* = \tilde{\tau}_{0.1}/2.3\mathrm{R}\cdot 10^3$ value, which will be referred to as the theoretical compensation parameter, where $\tau_{0.1}$ is the arithmetical mean of $\tau_{0.1}$.

Obviously, it may be expected that, the narrower the $T_{0.1}$ range considered, the better will be the linearity of a log Z *vs.* E plot. In order to test the validity of this presumption, a linear regression study was performed. The kinetic parameter values given in Table 3 were processed via linear regression in two approaches. In the first, all data were used. In the second, they were worked up separately for different $T_{0.1}$ ranges. Results are presented in Table 4, which also contains the correlation coefficient ρ, characterizing the linearity of the plot, the theoretical

Table 4 Kinetic compensation parameters

$T_{0.1}$ range / °C	ρ	b	a / mol·k^{-1}J^{-1}	a^* / mol·k^{-1}J^{-1}	Δ %
40–595	0.7739	–0.730	0.0831	0.0980	–15.23
40– 81	0.9934	–1.555	0.1503	0.1573	– 4.47
158–210	0.9988	–3.005	0.1111	0.1115	– 0.38
235–257	0.9997	–3.826	0.1067	0.1013	+ 5.31
355–390	0.9967	–4.882	0.0932	0.0815	+14.34
410–486	0.9970	–3.139	0.0703	0.0726	– 3.21
538–595	0.9941	–3.148	0.0620	0.0620	0.00

compensation parameter a^*, defined above, and the deviation Δ of the experimental parameter a from the theoretical one.

It is seen that when narrow temperature ranges are taken, the linearity becomes excellent, corresponding to $\rho > 0.99$. Meanwhile, the a values are quite near a^* strongly indicating the existence of an isokineic point not much differing from $T_{0.1}$. The only exception is observed in the interval $355°C < T_{0.1} < 390°C$, where the decomposition process becomes exothermal ($\Delta = +14.34\%$), which might be connected with the deviation of the actual sample temperature from the furnace temperature measured by means of the thermocouple.

Experimental

$H_2[PtBr_6]\cdot 6H_2O$. 5g of $H_2[PtCl_6]\cdot 6H_2O$ was dissolved in 20–25 ml of water and treated with 25 ml of 48% HBr and 1–2 ml of bromine, and the mixture was evaporated to dryness on a water bath. This operation was repeated 4–5 times, each time with 5 ml of conc. HBr and 1 ml of bromine.

$(\text{Amine}\cdot H)_2[PtBr_6]$. 20 mmol of the corresponding amine was treated with 10 ml of 20% HBr and the mixture was warmed for 10–15 minutes on a water bath. After cooling, the solution was treated with 2 mmol of $H_2[PtBr_6]$ in 10–15 ml of aqueous solution. After standing for 10–15 minutes, the crystalline salts that separated out were filtered off, washed with ice-cooled water and dried in the air.

The potassium and ammonium salts were also obtained by double exchange reactions with an excess of KCl or NH_4Cl.

Analysis

The platinum content was determined gravimetrically as metal after ignition at 800°–900°C. The nitrogen content was determined by means of the micro Dumas method.

Derivatographic measurements were performed with a MOM (Budapest) derivatograph. Sample weight: 200 mg. Heating rate: 5 deg/min. Atmosphere: static air. Reference material: α-Al_2O_3. Platinum crucible.

Differential scanning calorimetric measurements were made with a DuPont 990 Thermal Analyser (910 type DSC). Heating rate: 10 deg/min. Sample weight: 5–6 mg.

References

1 A. Gutbier and F. Bauriedel, Ber. Dtsch. Chem. Ges., 42 (1909) 4244.
2 L. Pigeon, Compt. Rend., 113 (1891) 476.
3 O. T. Christensen, J. Prakt. Chem., 23 (1881) 42.
4 A. Werner and K. Dawe, Ber. Dtsch. Chem. Ges., 40 (1907) 799.
5 J. Meyer and K. Kienitz, Z. Anorg. Allg. Chem., 242 (1939) 281.
6 J. Bellucci, Gazz. Chim. Ital., 33 (1903) 151.
7 W. Peters, Z. Anorg. Allg. Chem., 77 (1912) 175.
8 A. Gutbier, F. Bauriedel and C. J. Obermaier, Ber. Dtsch. Chem. Ges., 43 (1910) 3229.
9 A. Gutbier and A. Rausch, J. Prakt. Chem., 88 (1913) 413.
10 W. M. Delm and B. B. Wilcox, Amer. Chem. J., 35 (1906) 32.
11 A. Michaelis, Liebigs Ann. Chem., 320 (1902) 298.
12 L. Wöhler and F. Müller, Z. Anorg. Allg. Chem., 149 (1925) 378.
13 J. Zsakó, G. Liptay, Cs. Várhelyi and I. Ganescu, J. Thermal Anal., in press.
14 J. Zsakó, J. Thermal Anal., 15 (1979) 369.
15 J. Zsakó, M. Várhelyi and Cs. Várhelyi, J. Thermal Anal., 17 (1979) 123.
16 P. D. Garn, J. Thermal Anal., 10 (1976) 99.
17 A. J. Lesnikovich and S. V. Levchik, J. Thermal Anal., 30 (1985) 677.
18 J. Zsakó, J. Sztatisz, A. Czégeni, G. Liptay and Cs. Várhelyi, J. Thermal Anal., 32 (1987) 453.

Zusammenfassung — Es wurden die Kalium-, Ammonium- und dreizehn verschiedene Aminsalze von Hexabromoplatinsäure hergestellt und mittels Elementaranalyse charakterisiert. Mittels Derivatographie und DSC wurde die thermische Zersetzung dieser Komplexsalze untersucht. Das Wesen der Pyrolysevorgänge wird besprochen und mit dem der analogen Chlorokomplexe verglichen. Anhand der TG-Kurven wurden für verschiedene Schritte der thermischen Zersetzung kinetische Parameter ermittelt.